Subglass Relaxations. Intermolecular Packing and the Relaxation Times for Ester Side Group Reorientation: A Molecular Dynamics Simulation

Grant D. Smith and Richard H. Boyd*

Department of Materials Science and Engineering and Department of Chemical Engineering, University of Utah, Salt Lake City, Utah 84112

Received July 29, 1991; Revised Manuscript Received October 22, 1991

ABSTRACT: As a continuation of previous efforts to model subglass relaxation processes in flexible side group containing polymers, a molecular dynamics (MD) simulation study of side group rotation at subglass temperatures was performed. A model for the experimentally studied methyl acrylate/ethylene (MA/E) copolymer system was considered with the goal of examining intermolecular packing effects on the rotational energetics of the side group. Free energy barriers for the rotation of a MA side group in a polyethylene matrix, using an umbrella sampling technique, were generated for a number of MD-generated glass structures. Experimentally the distribution of relaxation times and accompanying activation energies is very broad. The distribution of rotational energy barriers determined from the MD study is also very broad and resembles closely the experimental distribution. The variations of barrier height are found to correlate with close-range packing effects in the glass.

Introduction

Relaxation processes that take place at temperatures well below the glass transition region are common in polymers and are important in determining material properties. The molecular mechanisms of these relaxations are not well understood but one important source is thought to be reorientation associated with flexible side groups. The homopolymers of vinyl acetate (VA) and methyl acrylate (MA) and their copolymers with ethylene (VA/E, MA/E) have previously been studied experimentally as models for such relaxations.[1-3] Work has also been carried out on developing molecular models for the subglass relaxations in these polymers.[4,5] There are two important general descriptors of relaxation processes. The first is the strength and this is a quasi-equilibrium property. That is, it represents the long-time limit of the change in value of the property being measured as the system relaxes. The second characteristic is associated with the kinetics of the process and is usually expressed as a distribution of relaxation times. Strengths vary widely for various subglass processes, and thus they are very diagnostic of underlying mechanisms. It follows that successful molecular models must be capable of explaining strengths. A molecular model has been presented for the strengths of the dielectric β processes associated with pendent ester group reorientation in the above-mentioned polymers.[4,5] The description is based on a statistical mechanical rotational isomeric state model for the isolated chains. The isolated chain picture is appropriate because it appears that the energies of the conformational states that govern relaxation strength are largely determined by intramolecular effects. By and large this model was successful in explaining the strengths, including the rather dramatic differences between the VA and MA type systems. The purpose of the present work was to address the other side of the problem, that is, the development of a model for the kinetic aspects that lead to the relaxation times.

Addressing the kinetics of the above subglass processes is a situation where intermolecular effects must be included. The barriers to reorientation of the side groups are clearly influenced by the hindrances presented by the matrix of surrounding chains. There are two general characteristics of the kinetics of all subglass relaxations. The first is that the dominant or central relaxation time appears to follow Arrhenius rather than WLF-Vogel-Fulcher temperature behavior. The second is that such processes are extremely broad in the time or frequency domain. The relaxation time distributions are much wider than those associated with glass transitions in amorphous polymers. A process as simple in concept as side group reorientation should be describable in terms of a site model. That is, the conformations of the side groups in their various orientations constitute sites. The strength model discussed above addressed determining the site energies for isolated chains, including all the various environments that arise as the result of various main-chain conformations and through varying comonomer environments. The relaxation times depend on the energetic barriers separating the sites. It is expected and confirmed[6] that the barriers resulting from *intra*molecular origin alone are too low to explain the experimental results. The *inter*molecular hindrances to reorientation contribute to the barriers and lengthen the relaxation times. This results in an increase in the central relaxation time. However, just as important as the effect on the average or central relaxation time is the effect on the distribution of times. The energetic differences in the various *intra*molecular environments for side group reorientation are insufficient to give rise to the very broad distribution that is found experimentally (this is commented on more fully below). Thus not only must the matrix contribute to increasing the barriers, but *local variations in the packing in the glass about individual reorienting groups must be sufficient to cause a significant variation in the overall barriers* if a site model description is to be successful. It is the effect of packing on the barriers, including the question of variation of packing environments, that is taken up in this work.

Molecular dynamics (MD) simulation was chosen as the method for studying the effect of packing. It should be understood that MD in its unadorned application is not an appropriate method. That is, following the time trajectories in the temperature region of interest, i.e., well below the glass temperature, will not result in the observation of side group rotations. The practical time scales (100 ps to 1 ns) for MD runs are far too short for accomplishing this. Raising the temperature will increase the rate of side group reorientation. However, experi-

0024-9297/92/2225-1326$03.00/0 © 1992 American Chemical Society

mentally it is observed in loss peak maps that the α glass–rubber region and the β subglass regions have merged at the MD time scales. An alternative is to compute, in the desired temperature region, free energy barriers to selected artifically induced conformational transitions via the "umbrella sampling" technique.[7] The key is "selected artificially induced" transitions. That is, the type of transition must be known. In the case of side group rotation this is straightforward. An artificial biasing or "window" potential can be used to force the transition of a selected rotationally flexible group from one stable position to another and thus to generate the free energy barrier for that group in its packing environment.[8-11] By repeating this procedure for a variety of individual selected groups, a collection of barriers for various packing environments can be generated. The packing environments can be generated by quenching MD structures generated at the higher temperatures associated with equilibration of structure over MD time scales. This is the strategy used in the present work.

The discrete set of activation energies obtained by examining several packing environments was compared to the distribution of activation energies calculated from experimental data for the example of the dielectric β process in a low MA content MA/E copolymer system.

Simulation Methodology

Basis for Comparison with Experimental Data. Complex plane analysis of dielectric relaxation data[1] for chemically dilute (<0.09 mole fraction MA) MA/E copolymers at several temperatures ranging from 110 to 190 K indicated that the data could be well represented by the Cole–Cole equation:[12]

$$\epsilon^*(\omega) = \epsilon_u + \frac{\epsilon_r - \epsilon_u}{1 + (i\omega\tau_0)^\alpha} \tag{1}$$

where ϵ^* is the complex dielectric constant, ω is the angular frequency, ϵ_r and ϵ_u are the relaxed and unrelaxed dielectric constants, respectively, τ_0 is the principal relaxation time, and α is the width parameter. The parameters ϵ_r, ϵ_u, τ_0, and α are all temperature dependent. The equations below were selected here as the average and representative of the temperature dependence of τ_0 and α for the β process in the four chemically dilute MA/E copolymers reported in ref 1

$$\log \tau_0 = 1948/T - 16.23 \tag{2}$$

$$\alpha = 0.212 + 0.00166(T - 133) \tag{3}$$

where T is the absolute temperature. The distribution of relaxation times F(ln τ) corresponding to Cole–Cole behavior can be expressed as[13]

$$F(\ln \tau) = \frac{1}{2\pi} \frac{\sin(\alpha\pi)}{\cosh[\alpha \ln(\tau/\tau_0)] + \cos(\alpha\pi)} \tag{4}$$

It is assumed here that the distribution of relaxation times results from a distribution of activation energies and that the entropies of activation are the same for each relaxation time. Thus an activation energy ΔH can be associated with each relaxation time τ. The apparent experimental validity of this will be commented on below. Therefore we write for the temperature dependence of relaxation time, τ

$$\ln \tau(T) = \Delta H(\tau)/RT + B \tag{5}$$

where $\Delta H(\tau)$ is the activation energy corresponding to τ, B is the same for all relaxation times, and R is the gas constant. Then, in terms of the principal relaxation time

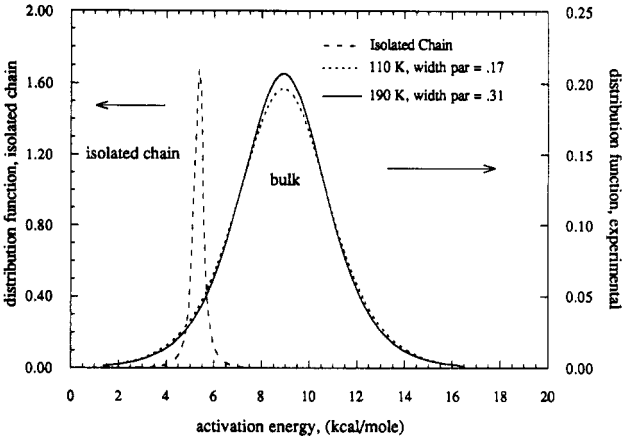

Figure 1. Experimental distribution of activation energies for the dielectric β process in bulk chemically dilute MA/E copolymers, calculated under the assumption that the entropy of activation is the same for all relaxation times. Two curves are shown, one calculated from the experimental Cole–Cole width parameter at 110 K and the other at 190 K. Also shown is a distribution of rotational energy barriers for an isolated chain MA side group. It is based on barriers calculated for a number of the most populated chain conformations.

of eqs 1 and 2

$$\ln(\tau/\tau_0) = (\Delta H(\tau) - \Delta H(\tau_0))/RT \tag{6}$$

Since there is a unique correspondence between τ and $\Delta H(\tau)$, the latter can be considered as the independent variable in eq 4 and written simply as ΔH, or from F(ΔH) dΔH = F(ln τ) d ln τ, then

$$F(\Delta H) = \frac{1}{2\pi RT} \frac{\sin(\alpha\pi)}{\cosh(\alpha(\Delta H - \Delta H_0)/RT) + \cos(\alpha\pi)} \tag{7}$$

and where from eq 2 the experimental principal activation energy ΔH_0 of the process is 8.9 kcal mol^{-1}.

Experimentally it is found, eq 3, that the width parameter, α, is temperature dependent. The process narrows with increasing temperature. However, if the assumption about the distribution of relaxation times being solely due to a fixed distribution of activation energies is valid, then then the distribution computed from eq 7, with α from eq 3, should be independent of temperature. The test of this is shown in Figure 1, where the calculated distribution of activation energies for the chemically dilute MA/E copolymer system is displayed at 110 and 190 K. The latter are the experimental temperature limits of eqs 2 and 3. It may be seen that the distribution is nearly temperature independent. This is in spite of the fact that the Cole–Cole width parameter has nearly doubled over the temperature range studied. Conversely, it may be said that the experimentally observed process-narrowing with increasing temperature is a simple consequence of the temperature dependence of the relaxation times of the type expressed in eq 5 and a temperature-independent distribution, F(ΔH).

The distribution, F(ΔH), for bulk polymer of Figure 1 forms the basis for comparison of the simulation results with experiment. This comparison is somewhat complicated by the following issue. The interpretation of the experimental dielectric β relaxation in MA/E copolymers given previously[1,2] proposes that the process is actually a composite of two mechanisms. One of them is the side group reorientation process considered here. The other is rigid side group excursions driven by main-chain reorientations connected with the PE γ process. It is not possible to separate their relative contribution to the

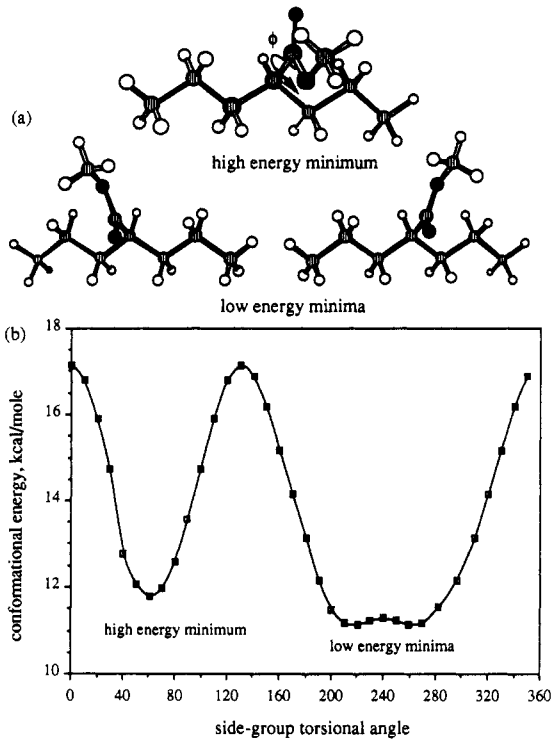

Figure 2. Methyl acrylate side group. (a) Molecular geometry of the low-energy side group states for a MA group containing model molecule. Atoms outlined in bold define the side group torsional angle. This torsional angle is the reaction coordinate in the MD umbrella sampling simulations. (b) Conformational energy as a function of side group torsional angle for the model (isolated) molecule conformation shown in (a).

relaxation time distribution except to make an estimate of the relative relaxation strengths of the two mechanisms. In vinyl acetate copolymers with ethylene (VA/E) the two processes are experimentally partially resolved into observable β and γ loss peaks.[2,3] The observed strength of the composite β process in MA/E copolymers is ~3–4 times greater than the observed γ process in VA/E polymers at the same polar group content.[1,2] Since main-chain-driven rigid ester group excursions are presumed as the basis of the γ process contributions in both polymer types, it is a reasonable presumption that the γ mechanism contribution to the composite β process in MA/E is similar to the observed strength of the γ process in VA/E. On this basis the side group rotational mechanism contributes several times as much to the measured strength as the main-chain γ mechanism. Thus we will assume here that the distribution in Figure 1 is sufficiently dominated by the side group rotation mechanism that comparison of the simulation results can be made directly with it.

Isolated Chain. Isolated chain molecular mechanics studies of PMA and MA/E copolymers have been described elsewhere.[4–6] In these studies the β process in these polymers was considered to be due to rotation of the MA side groups between low-energy torsional states. Figure 2a shows the molecular geometry of the three side group energy minimum states for a MA/E model molecule for a specific main-chain conformation. The energetics for rotation between the states for this model are shown in Figure 2b. By computing conformational energy curves similar to Figure 2b for highly populated conformations of the model molecule, it is possible to calculate a distribution of rotational energy barriers for side group rotation resulting from local chain conformational differences.[6] The resulting distribution is shown in Figure 1. The isolated chain distribution is much narrower than the experimental distribution. Further, the principal activation energy of 5.3 kcal/mol is significantly smaller than the experimental value of 8.9 kcal/mol.

MD Umbrella Sampling Formalism. Let $\rho(\phi)$ be the relative probability of configurations with a given value of the reaction coordinate ϕ in a canonical ensemble of the remaining coordinates.[11] In our case the reaction coordinate ϕ is the torsional angle of the side group as shown in Figure 2a. The potential of mean force $A(\phi)$, or Helmholtz free energy, associated with $\rho(\phi)$ is given by the expression

$$A(\phi) = -k_B T \ln \rho(\phi) \tag{8}$$

where k_B is the Boltzmann constant and T is the absolute temperature. If a molecular dynamics simulation of adequate length to sample all values of ϕ were possible, a single run would be sufficient to completely determine the rotational energetics of the side group. Unfortunately, the relatively short trajectories (up to ~1 ns) of MD simulations as compared to the relaxation time (>10^4 ns at subglass temperatures) of the process preclude adequate sampling of high-energy configurations. This limitation can be circumvented by use of the umbrella sampling technique, where the probability of finding the side group in a certain desired range of ϕ is increased by use of a biasing window potential, $U^*(\phi)$.[7,11,14] It is simply shown[11] that the biased probability density $\rho^*(\phi)$, in the presence of the window potential, is related to the unbiased value by the expression

$$\rho^*(\phi) = e^{-\beta U^*(\phi)} \langle e^{-\beta U^*(\phi)} \rangle^{-1} \rho(\phi) \tag{9}$$

where β is $(k_B T)^{-1}$ and the brackets indicate the unbiased canonical ensemble average. With eq 9, eq 8 becomes

$$A(\phi) = -k_B T \ln \rho^*(\phi) - U^*(\phi) - C_i \tag{10}$$

where

$$C_i = k_B T \ln \langle e^{-\beta U^*(\phi)} \rangle \tag{11}$$

When overlapping windows are used, resulting Helmholtz free energy curves can be shifted to form a single, continuous curve, thereby eliminating the need to explicitly evaluate the constants C_i.

System Simulated. The system consists of a single MA type pendent ester group in an ethylene chain surrounded by a matrix of polyethylene segments (Figure 3). It is customary in MD simulations, in order to reduce computer time, to contract the hydrogen atoms into the carbon atoms as "united atom" centers. Specially calibrated 6–12 power nonbonded potentials have been developed for the purpose. In general, in molecular mechanics force fields, effective torsional potentials for bond rotation depend both on the potential function explicitly parameterized in terms of the torsional angle and on the nonbonded potentials. For example, in a methylene chain with explicit hydrogens rather than contracted united atom centers, the explicit torsional potential is taken as a threefold cosine function of the rotational angle. Part of the effective barrier and the gauche–trans energy difference results from the nonbonded interactions between explicit atoms. In general, the united atom nonbonded potentials do not do a good job in the intramolecular context of barriers and conformation energy differences. This is overcome by switching off the four- or even five-center intramolecular interactions and directly parameterizing the torsional potential with additional terms. For example, a single-fold torsional angle cosine term is commonly used to represent the gauche–

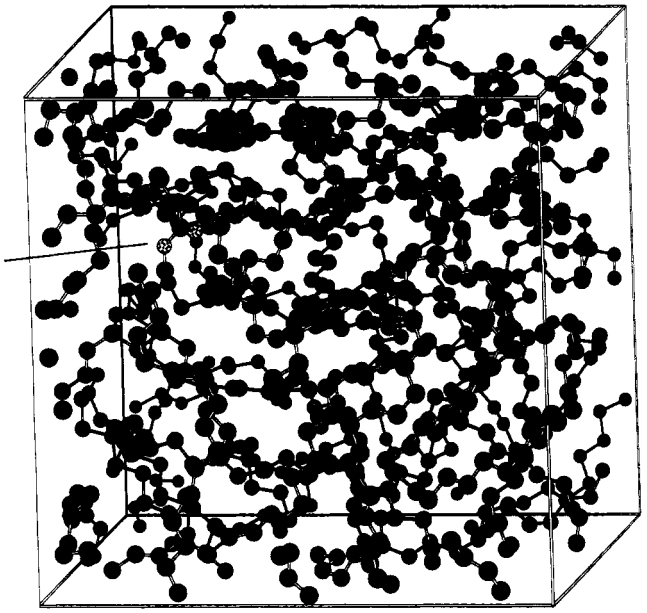

Figure 3. System simulated: A single MA type ester group (at pointer) on a C_{24} hydrocarbon chain surrounded by a matrix of polyethylene. In the simulation the ester group containing chain has explicit hydrogens (not shown). The ester group interacts with explicit (virtual) hydrogens and carbons in the matrix. Matrix–matrix nonbonded interactions are of the united-atom contracted-hydrogen methylene bead type.

trans energy difference. In the present more complicated case of an ester group containing various atom types, it would be very difficult to carry out this parameterization and have confidence in its reliability. Thus we have designed the simulation procedure in such a way as to permit use of the explicit hydrogen atom formulation for the ester group but permit the united atom contraction for the much more numerous methylene groups in the matrix.

The system considered consists of two chains. One chain is comprised of 24 main-chain carbons with explicit hydrogens and a methyl acrylate side group attached to the 13th carbon. The explicit atom force field including realistic nonbonded, stretch, bend, and torsional functions used previously[15,16] was employed intramolecularly in this chain. The other chain, representing the matrix, consists of a single polyethylene chain of 744 main-chain carbons. Within the matrix including all matrix–matrix nonbonded interactions, the centers were considered to be united atom methylene beads, where a methylene unit was considered to be a single force center. The nonbonded, stretch, bend, and torsional functions for methylene beads used previously[17] were employed. In intermolecular nonbonded interactions between the ester group and the matrix polyethylene, explicit hydrogens were considered. This was accomplished by placing "virtual" hydrogens at each matrix carbon center considered and computing the interaction from the explicit atom nonbonded potential set. The virtual hydrogens do not participate in the dynamics and transfer of the forces to the matrix carbon centers via constraint equations as described below. Intermolecular interaction between non-ester group methylene centers in the C_{24} chain and the matrix were considered to be united atom methylene bead interactions.

The constraints involving the virtual hydrogens discussed above were formulated as follows. If $\mathbf{r}_1$ and $\mathbf{r}_2$ are the main-chain bond vectors about the attachment point, the hydrogens are taken to lie in the plane containing the vectors $\mathbf{r}_1 - \mathbf{r}_2$ and $\mathbf{r}_2 \times \mathbf{r}_1$, with fixed bond lengths and angles with respect to the $\mathbf{r}_1 - \mathbf{r}_2$ vector. With the positions of the hydrogens so formulated (yielding constraint equations), it is straightforward to calculated the change in position of the hydrogen with respect to a change in position of the three base carbon atoms. This can be formulated in terms of 3 (3 × 3) Jacobian matrices $\mathbf{J}_C$, $C = i-1, i, i+1$, one for each of the three base atoms about the chain attachment point, i, of the virtual hydrogen, v. With respect to one of the base atom displacements, $\Delta\mathbf{q}_C$, the virtual hydrogen displacement, $\Delta\mathbf{q}_v$, is

$$\Delta\mathbf{q}_v = J_C \Delta\mathbf{q}_C \tag{12}$$

where $\mathbf{q}$ is a Cartesian coordinate vector. It is now simple to redistribute any force acting on a virtual hydrogen ($\mathbf{F}_{vj}$) from a distant center, j, to forces on base beads ($\mathbf{F}_{Cj}$).[18] The forces are

$$\mathbf{F}_{vj} = -\frac{\partial U(r_{vj})}{\partial \mathbf{q}_v} \tag{13}$$

$$\mathbf{F}_{Cj} = -\frac{\partial U(r_{Cj})}{\partial \mathbf{q}_C} = -\frac{\partial U(r_{vj})}{\partial \mathbf{q}_v}\frac{\partial \mathbf{q}_v}{\partial \mathbf{q}_C} = \mathbf{F}_{vj}\mathbf{J}_C \tag{14}$$

where $U(r_{vj})$ is the potential energy of the virtual hydrogen–jth center interaction.

Periodic boundary conditions were employed, and velocity Verlet integration of the equations of motion was used. Trajectories were calculated at constant temperature by rescaling the velocities at each time step by a coefficient γ given by[19]

$$\gamma = \left(1 + \frac{\delta_t}{t_T}\left(\frac{T_0}{T} - 1\right)\right)^{1/2} \tag{15}$$

where T_0 is the fixed temperature, T is the current kinetic temperature, t_T is the temperature rescale time constant, and δ_t is the integration time step constant. Values of 500 and 0.5 fs, respectively, were used for the time constants.

Generation of Glass Structures. The procedure used to generate new glass morphologies was as follows. A 25-ps trajectory beginning with an equilibrated melt configuration at 500 K generates a "new melt" configuration. The autocorrelation function for torsional angles has completely decayed in this time. The 500 K "new melt" is quenched to 300 K over 8 ps. A 25-ps equilibration trajectory is performed on the 300 K melt, after which time the system energy is stable. It is then quenched over 8 ps to 200 K. A final 25-ps trajectory yields an equilibrated "glass" at 200 K that is also stable with respect to total energy. The system was determined to be a glass at 200 K on the time scale of the MD runs due to the infrequency of torsional transitions (~0.04 conformational transitions/bond in 10 ps) and the small decrease in the internal rotation angle autocorrelation function (to ~0.98 after 10 ps), where 10 ps corresponds to a typical umbrella sampling run for a given window potential (see below). This temperature also corresponds to the upper end of the range of experimental relaxation data for the process. The volume at each temperature was chosen to yield a density for the periodic system which corresponds to the experimental values for amorphous polyethylene.[17] The volume is reduced proportionally for each time step during the quenches.

Free Energy Calculations. Previous investigations[11] have employed the device of constraining the structure outside a sphere of an fixed radius centered at the moiety of interest (i.e., the rotating side group) during umbrella sampling MD trajectories. This greatly reduces calculation time as the forces between constrained particles need not be calculated. Of additional importance is the fact that

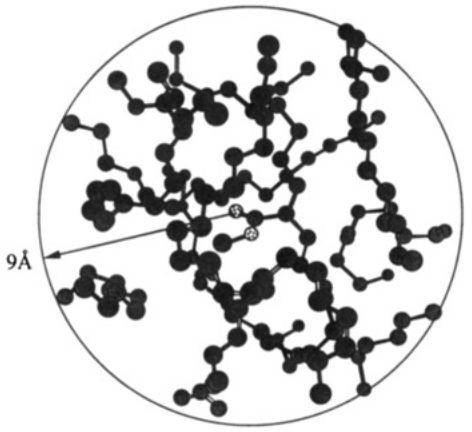

Figure 4. Configuration of unconstrained atoms about the rotating side group in a typical glass structure.

energy fluctuations outside of the region of interest are eliminated by the constraints and smoother energy barriers are obtained. We have adopted this scheme, and a sphere radius of 9 Å was chosen as illustrated in Figure 4. This radius was large enough that constraints did not affect the rotational energetics of the side group and corresponded to the nonbonded cutoff distance.[17] Forces between unconstrained atoms (the ~150 atoms, including explicit hydrogens, lying within the sphere) and constrained atoms (those outside the sphere) were still considered.

The window potential for umbrella sampling was of the form

$$U^*(\phi) = \chi(\phi - \phi_0)^2 \qquad (16)$$

where a value for χ of 20 kcal/mol was determined to be optimum for allowing adequate overlap for windows 15° wide. The procedure for umbrella sampling was as follows:

(1) Increment ϕ_0 to a new value (15° increments were used in general).

(2) Perform a 10-ps trajectory to allow the system to equilibrate to the new window potential. The side group torsional angle is periodically sampled.

(3) Perform a 10-ps sampling trajectory.

(4) Repeat step 3 if the probability density functions resulting from steps 2 and 3 differ significantly.

Results

Figure 5 shows typical probability densities as calculated for three overlapping windows. Application of eq 10 and joining of the resulting free energy curves into a continuous function yield the free energy curve also shown in Figure 5. The free energy curve for a complete rotation in the bulk is shown in Figure 6. Also shown is the conformational energy curve determined by energy minimization of an all-trans isolated chain MA/E model molecule (see Figure 2b). The starting location for the side group in the bulk simulation is also indicated. The contribution of the matrix to the effective barrier for reorientation is apparent. It is also apparent that the relative energies of the energy minimum states are affected in the simulation by the amorphous packing. That is, the side group does not find a new minimum unaffected by the packing. This effect will be considered in detail later.

Figure 7 is a comparison of the free energy rotational barrier and the potential energy rotational barrier for the same glass structure. The latter is obtained by sampling the potential energy from the biased configurations.[11] The similarity of the curves implies that there is no significant entropic contributrion to the rotational energy barrier, at least for the path found by the simulation. Application of transition state theory to the experimental principal relaxation time for the PMA homopolymer dielectric β process[1] also indicates minimal entropic contribution to the free energy barrier. However, for the MA/E case as represented by eq 2, a positive activation entropy of ~16 cal K^{-1} mol^{-1} is indicated. This is substantial and no indication of this is seen in the results of Figure 7. It is not surprising that the simulation curves such as in Figure 7 do not indicate an appreciable entropy of activation. In the picture envisioned, a thermally activated barrier crossing, entropic effects would be associated with vibrational frequency differences in the ground and activated states. These effects are usually rather modest. The similarity of the MD free energy and energy results is

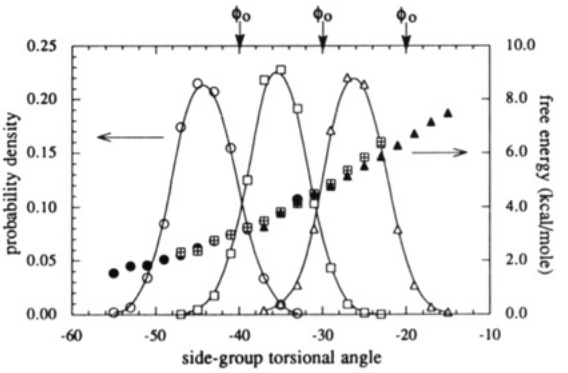

Figure 5. Illustration of umbrella sampling. Sampled probability densities $\rho^*(\phi)$ for three window potentials (whose centers are indicated at the top of the figure), left-hand ordinate. Also shown (right-hand ordinate) is the free energy derived by shifting $A(\phi) + C_i = -k_B T \ln \rho^*(\phi) - U^*(\phi)$ from eq 10 to obtain overlapping curves. A complete free energy curve as in Figure 6 uses additional overlapping windows to span the complete torsional angle range.

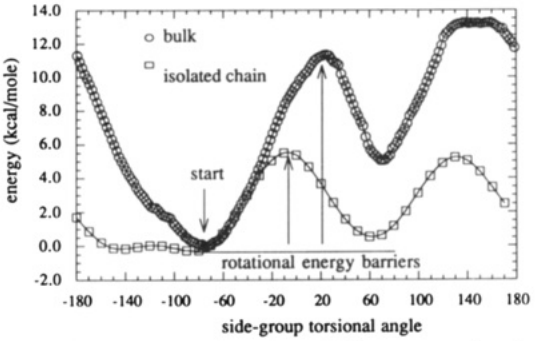

Figure 6. Free energy as a function of side group torsional angle for a complete rotation in the bulk glass. Also shown is the conformational energy vs side group torsional angle for an isolated chain side group rotation (Figure 2b).

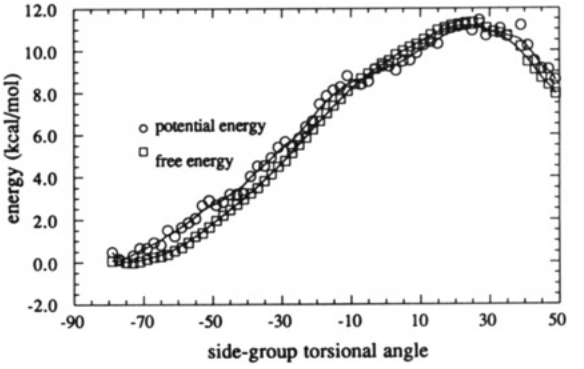

Figure 7. Free energy and potential energy compared as a function of side group torsional angle over a rotational energy barrier in the bulk.

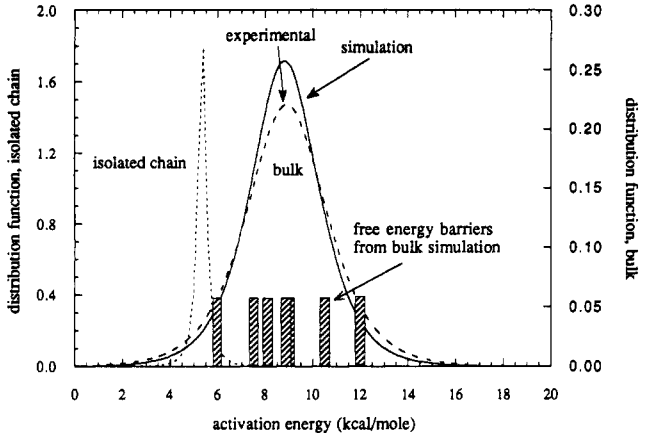

Figure 8. Rotational energy barriers for side group rotation computed for seven glass structures (shaded bars). Also shown (dashed curve) is the experimental distribution of activation energies (190 K) from Figure 1. The full curve corresponds to a Cole–Cole distribution of activation energies that has the same average activation energy and standard deviation as the discrete set of seven computed in the bulk and shown as shaded bars.

Table I
Comparison of Experimental and Calculated Distribution of Activation Energies

	exptl	modeling	
		bulk	isolated chain
$E_a°$ or $\langle\Delta G\rangle$,[a] kcal/mol	8.9	8.8	5.4
σ,[b] kcal/mol	2.12	1.84	0.35
α[c] (190 K)	0.31	0.35	0.86

[a] Principal activation energy or free energy. [b] Standard deviation of the activation energy distribution. [c] Cole–Cole width parameter value, determined in the case of modeling as the value required to produce the standard deviation of the activation energy distribution found from simulation.

consistent with this, and, as stated, the experimental results for MA homopolymer are as well. The question of why the MA/E copolymer experimental results indicate a significant entropy of activation can only be speculated on. It was presumed above, in the section on basis for comparison with experiment, that the experimentally observed β process is a composite of the side group rotation process and a main-chain polyethylene-like γ process. It was argued that the strength is dominated by the side group rotation. It may be, however, that "contamination" from the γ-like main-chain process has more of an effect on the entropy of activation than supposed.

Distribution of Activation Energies. The effect of the amorphous bulk packing on the average rotational energy barrier and the distribution of rotational energy barriers was considered by examining a number of glass structures. A total of seven structures were generated and examined through the umbrella sampling technique. Rotational energy barriers for each are shown in Figure 8. In addition to the experimental distribution at 190 K and the isolated chain distribution, a curve, labeled simulation, is displayed. This distribution function is the Cole–Cole distribution yielding the same principal (mean) value and standard deviation as the seven discrete bulk simulation values. Table I shows a comparison of principal activation energies, standard deviations of the activation energy distributions, and Cole–Cole width parameter values for experiment, bulk simulation, and the isolated chain model. The bulk simulation results indicate that variations in the amorphous packing environment of the side groups lead to a broad distribution of rotational energy barriers that resembles the experimental distribution of

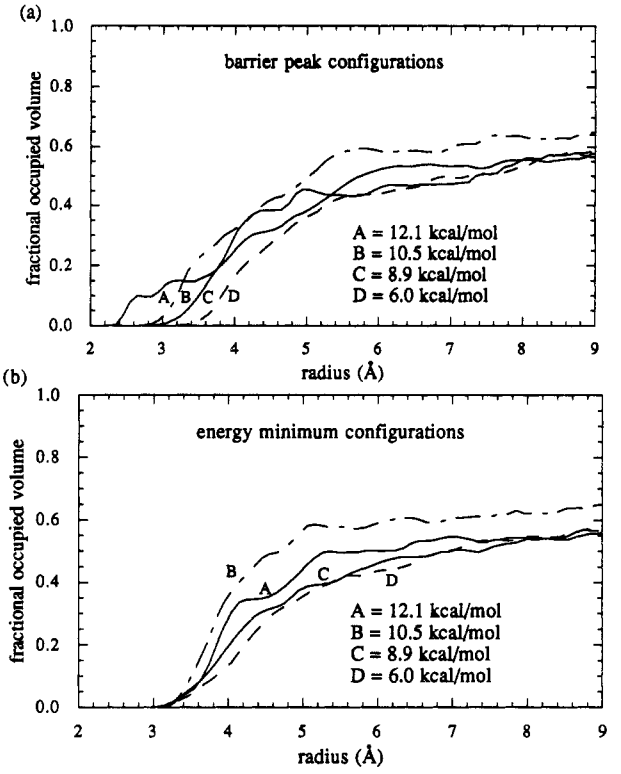

Figure 9. Correlation of local packing density with barrier height. (a) Fractional occupied volume surrounding the side group for barrier peak configurations of the side group as a function of distance away from the side group. Results for four glass structures labeled according to the height of the barrier found in each. (b) Fractional occupied volume surrounding the side group for energy minimum configurations of the side group.

activation energies and yields a principal activation energy similar to experiment.

Local Structure. It is of interest to examine the glass morphology local to the side group in order to see how differences in packing affect the rotational energy barrier. One method of investigating packing is to calculate the occupied volume distribution $f_0(r)$ around an atom, which can be defined as[20]

$$f_0(r) = \frac{4\pi v_s \rho_n \int_{r_c}^{r} r^2 g(r)\, dr}{v_{shell}(r)} \tag{17}$$

where r is the radial distance from the center of the atom of interest, v_s is the occupied volume/atom determined by Monte Carlo sampling of snapshots of the system,[17] $g(r)$ is a radial distribution function about the atom of interest, r_c is half of the Lennard-Jones hard-core diameter, and

$$v_{shell}(r) = \frac{4\pi(r^3 - r_c^3)}{3} \tag{18}$$

The occupied volume distribution indicates what fraction of a shell of outer radius r and inner radius r_c is occupied by other atoms. Typical results for configurations where the side group is at the rotational energy barrier peak are shown in Figure 9a. Results for configurations where the side group in the energy minimum state are shown in Figure 9b. The curves represent averages of the fractional occupied volume distributions for the side group methyl carbon, carbonyl oxygen, and ether oxygen. Examination of Figure 9 reveals a correlation between the short-range packing density around the side group in the barrier peak configurations and the magnitude of the rotational energy barrier. Beyond 4–5 Å the correlation dies off. The matrix contribution to the rotational energy barrier appears to be primarily a function of the short-range nonbonded

interactions of the side group with matrix as the side group crosses the rotational energy barrier and is independent of longer range density fluctuations in the glass. No correlation between short-range packing density and rotational energy barrier is seen for the starting configurations near the rotational energy minimum. Indeed, the short-range nonbonded interactions appear to be very similar for the energy minimum configurations for all examined glass structures.

Relative Site Energies. A fundamental assumption in the isolated chain RIS modeling of the relaxation strength of the dielectric β process in MA and MA/E copolymers is that the relative energies of the energy minimum torsional states or sites of the methyl acrylate side groups are not influenced by the glass matrix or packing.[4,5] Examination of Figure 6 indicates that, in the bulk simulation, this assumption does not hold. The energy minimum found in the bulk on rotation over the barrier is significantly higher in energy relative to the starting point than found in the isolated chain. That is, after moving over the barrier the rotating group fails to find a new site as favorably packed intermolecularly as the starting point. This result must be largely nonphysical for the following simple reason. If it were so, then reorientation of flexible groups would generally involve large site energy differences. It follows from this that, due to unfavorable Boltzmann weighting, the populations of the alternative sites would be very small and the strengths of associated relaxations would be very weak and essentially nonobservable.[5] The experimental strengths of such processes, including the case studied here, are often quite substantial. Below, some comments are made that are directed toward rationalizing this aspect of the simulation results.

First, it is necessary to consider differences in experimental glass formation and glass formation in the simulation. A real quench from a 300 K melt to a 200 K glass occurs on a time scale on the order of seconds, during which the side group will undergo many millions of transitions between low-energy sites. The side group will spend an appreciable fraction of the time in each of the energy minimum states and very little time at the top of the energy barrier. For a simulated quench, the time scale is so short as to preclude a reasonable chance of a side group transition occurring. The side group spends all of its time in a relatively narrow range of torsional angles about an energy minimum state, labeled "start" in Figure 6. A reasonable supposition therefore follows. During a real quench the side group spends an appreciable fraction of its time in each side group state, thereby clearing a space for itself in the matrix about each potential site. During a simulated quench, the side group spends all of its time in a single energy minimum state, allowing for artificially close packing in the other potential sites. This supposition is supported by Figure 9. It can be seen that in configurations where the side group is located in the same state as during quenching (Figure 9b), the short-range packing is essentially independent of the particular glass structure. This implies that the side group does indeed clear out a space for itself in the matrix. Figure 9a shows configurations where the side group is well removed from its position during quenching. The short-range packing varies greatly and is in general more dense than that for the configurations shown in Figure 9b.

There is another related consequence of the amount of time spent in each site in physical systems compared to the length of the simulations. Barrier crossing is physically rapid and the MD sampling time scale is appropriate for this part of the transition. But it is possible that the higher site energy found in the second state would be considerably lower, though slower structural rearrangement, if the MD runs were much longer at the second minimum. Physically, the time spent at the minima would be appropriate to this but it is practically precluded by computation time.

In addition to the general comment at the beginning of this section about the observation of such subglass process, more direct experimental evidence exists to support the supposition that the relative site energies are not greatly affected by the glass matrix. A study of the effect of absorbed water on the dielectric β process in PVAc has been performed.[3] PVAc is very similar to PMA in molecular structure, and the strength of the dielectric β process in PVAc and VA/E copolymers can be represented well by a site model involving side group rotation that is completely analogous to the model for MA and MA/E.[5] The study indicates that water acts as a plasticizer for the dielectric β process, apparently agglomerating near the homophillic ester side groups. The time–temperature location of the process and activation energy are somewhat sensitive to water content. The width of the process is more sensitive to water content, becoming narrower as water content increases. However, the strength of the process is experimentally essentially independent of water content. Apparently water alters the influence of the matrix on the rotational energy barrier (i.e., the packing near the side group in barrier peak side group configurations) but does not affect the relative energies of the local minimum energy states. This implies in turn that the matrix has little effect on the relative energies of the minimum energy sites.

Acknowledgment. We are indebted to the Polymers Program, Division of Materials Research, National Science Foundation, for financial support and to the Utah Supercomputing Institute, where the computations were done.

References and Notes

(1) Buerger, D. E.; Boyd, R. H. *Macromolecules* **1989**, *22*, 2694.
(2) Buerger, D. E.; Boyd, R. H. *Macromolecules* **1989**, *22*, 2699.
(3) Smith, G. D.; Liu, F.; Devereaux, R. W.; Boyd, R. H. *Macromolecules*, in press.
(4) Smith, G. D.; Boyd, R. H. *Macromolecules* **1991**, *24*, 2725.
(5) Smith, G. D.; Boyd, R. H. *Macromolecules* **1991**, *24*, 2731.
(6) Smith, G. D. Ph.D. Dissertation, University of Utah, 1990.
(7) Valleau, J. P.; Torrie, G. M. In *Statistical Mechanics*; Berne, B. J., Ed.; Plenum: New York, 1977; Part A, pp 169–194.
(8) Gelin, B. R.; Karplus, M. *Proc. Natl. Acad. Sci. U.S.A.* **1975**, *72*, 2002.
(9) McCammon, J. A.; Karplus, M. *Biopolymers* **1980**, *19*, 1375.
(10) McCammon, J. A.; Lee, C. Y.; Northrup, S. H. *J. Am. Chem. Soc.* **1983**, *105*, 2232.
(11) Northrup, S. H.; Pear, M. R.; Lee, C. Y.; McCammon, J. A.; Karplus, M. *Proc. Natl. Acad. Sci. U.S.A.* **1982**, *79*, 4035.
(12) Cole, K. S.; Cole, R. H. *J. Chem. Phys.* **1941**, *9*, 341.
(13) McCrum, N. G.; Read, B. E.; Williams, G. *Anelastic and Dielectric Effects in Polymeric Solids*; Wiley-Interscience: New York, 1967.
(14) Rebertus, D. W.; Berne, B. J.; Chandler, D. *J. Chem. Phys.* **1979**, *70*, 3395.
(15) Sorensen, R. A.; Liau, W. B.; Kesner, L.; Boyd, R. H. *Macromolecules* **1988**, *21*, 200.
(16) Smith, G. D.; Boyd, R. H. *Macromolecules* **1990**, *23*, 1527.
(17) Boyd, R. H.; Pant, K. *Macromolecules* **1991**, *24*, 4078.
(18) VanGunsteren, W. F.; Boelens, R.; Kaptein, R.; Scheek, R. M.; Zuiderweg, E. R. P. In *Molecular Dynamics and Protein Structure*; Hermans, J., Ed.; University of North Carolina Printing Department: Chapel Hill, NC, 1985; pp 92–99.
(19) Berendsen, H. P. C.; Postma, J. P. M.; VanGunsteren, W. F.; Di Nola, A.; Haak, J. R. *J. Chem. Phys.* **1984**, *84*, 3684.
(20) Takeuchi, H.; Roe, R. J.; Mark, J. E. *J. Chem. Phys.* **1990**, *93*, 9042.